

Enhanced Performance of Quantum Dots Sensitized Solar Cell Utilizing Copper Indium Sulfide and Reduced-Graphene Oxide with the Presence of Silver Sulfide (Peningkatan Prestasi Sel Suria Dipekakan Titik Kuantum menggunakan Tembaga Indium Sulfida dan Grafin Oksida Terturun dengan Kehadiran Perak Sulfida)

NURUL SYAFIQAH MOHAMED MUSTAKIM, MUHAZRI ABD MUTALIB, SUHAILA SEPEAI, NORASIKIN AHMAD LUDIN, MOHD ASRI MAT TERIDI & MOHD ADIB IBRAHIM*

ABSTRACT

In this study, rGO/CuInS₂ has been successfully prepared onto TiO₂ thin film using solvothermal method followed by Ag₂S deposition layer by successive ionic layer adsorption and reaction deposition (SILAR) technique. The morphology, structural, and optical properties of TiO₂/rGO/CuInS₂ thin film were investigated by using field emission scanning electron microscopy (FESEM), energy-dispersive X-ray spectroscopy (EDX), atomic force microscope (AFM), X-ray diffraction (XRD) and ultra-violet-visible near infrared spectrophotometer (UV-Vis). For electrical properties, electrochemical impedance spectra (EIS) and current-voltage (I-V) test investigated the interfacial charge-transfer resistances and the conversion efficiency of the samples. Results showed that the average particles size of the samples ranged from ±46.52 to ±53.97 nm in diameter. UV-VIS analysis indicated that TiO₂/rGO/CuInS₂ thin film showed better light absorption capability with the presence of Ag₂S deposition layers. The rGO/CuInS₂ quantum dot sensitized with Ag₂S layers exhibit a photovoltaic power conversion efficiency of 0.33%, which has great improvement of short circuit current (I_{sc}) comparing with that of rGO/CuInS₂ quantum dot sensitized without Ag₂S deposition layers.

Keywords: Ag₂S; CuInS₂; quantum dots; rGO; SILAR; solar cells; solvothermal

ABSTRAK

Dalam kajian ini, rGO/CuInS₂ telah berjaya disediakan ke atas filem nipis TiO₂ dengan menggunakan kaedah solvoterma diikuti dengan lapisan pemendapan Ag₂S melalui teknik penjerapan dan tindak balas lapisan ion berturut-turut (SILAR). Sifat morfologi, struktur dan optik bagi filem nipis TiO₂/rGO/CuInS₂ dikaji dengan menggunakan mikroskopi elektron imbasan bidang (FESEM), spektroskopi sinar-X penyebaran tenaga (EDX), mikroskop kekuatan atom (AFM), difraksi sinar-X (XRD) dan spektrofotometer dekat inframerah ultraungu boleh nampak (UV-VIS). Untuk sifat elektrik, ujian elektrokimia impedansi spektra (EIS) dan arus-voltan (I-V) mengkaji rintangan pemindahan cas antara muka dan kecekapan penukaran sampel. Hasil kajian menunjukkan bahawa ukuran purata bagi sampel hablur adalah berkisar antara ± 46.52 hingga ± 53.97 nm. Analisis UV-VIS menunjukkan bahawa filem nipis TiO₂/rGO/CuInS₂ menunjukkan keupayaan penyerapan cahaya yang lebih baik dengan adanya lapisan pemendapan Ag₂S. Titik kuantum terpeka rGO/CuInS₂ dengan lapisan Ag₂S menunjukkan kecekapan penukaran kuasa fotovoltan sebanyak 0.33%, yang mempunyai peningkatan arus litar pintas (I_{sc}) yang besar berbanding dengan titik kuantum terpeka rGO/CuInS₂ tanpa lapisan pemendapan Ag₂S.

Kata kunci: Ag₂S; CuInS₂; rGO; sel suria; SILAR; solvoterma; titik kuantum

INTRODUCTION

The range of materials and structures of solar cells is very important to achieve good photovoltaic devices (Kouhnavard et al. 2014). Due to its extra-ordinary properties, graphene shows promising applications in many fields such as photovoltaic devices, nano-

electrochemical systems, nanoelectronics, and mechanical alloying (Ubani et al. 2016; Zhang et al. 2015a). Basically, graphene is a mono-layer structure of two-dimensional graphite which makes it an ideal material to has the ability as a larger donor-accepter interface with quantum dots (QDs) material. Besides, since the work function

of this semi metallic graphene is 4.5 eV, it is capable of dissociating excitons that generated in the QDs (Kumari et al. 2014). It is highly transparent as well as able to absorb 2.3% of incident white light which making it highly suitable for photo anode applications in solar cell devices (Madhavan et al. 2012). According to Kumari et al. (2014), the presence of graphene in photovoltaic applications are likely to produce better stability of the devices.

The application of CuInS₂ QDs in photovoltaic application have already been studied due to its unique properties such as non-toxicity material and high absorption coefficient. There are various synthesis methods including solid state reaction, hot injection method, chemical bath deposition, solvothermal and SILAR technique have been applied to prepare CuInS₂ nanostructures (Hosseinpour-Mashkani et al. 2014, Mustakim et al. 2018). However, the power conversion efficiency the current CuInS₂ based QDSSCs is still low and not satisfactory for practical application to be commercialized.

On the other hand, introduction of passivation layer in QDSSCs has been proved can help to enhance the performance of solar cells (Peng et al. 2014). Thin layer that passivate the QDs could improve QDs stability and promote electron injection from the QDs to the photo anode. It can also prevent leakage of current from the QDs to electrolyte, which can enhance the performance of QDSSCs. According to Holi et al. (2017), Ag₂S is one of the best materials to be used in solar cells since it is environmentally benign material. In addition, Ag₂S has a large absorption coefficient and a direct band gap of 0.9 to 1.05 eV which is equal to the optimal band gap of 1.13 eV for a photovoltaic device (Tubtimtae et al. 2010).

Therefore, the aim of this study was to investigate the performance of the CuInS₂ quantum dot and rGO with and without the presence of Ag₂S as interface layer on the QDSSCs. The morphology, structural, optical, and electrical properties of nanostructured CuInS₂ QDs and the rGO as an effective photosensitizer and the presence of Ag₂S layers in solar cell were carried out during the investigation. From this study, the optimum performance of environment friendly TiO₂/rGO/CuInS₂/Ag₂S thin films can be applicable as a photoanode for QDSSCs.

MATERIALS AND METHODS

MATERIALS

All reagents including hydrochloride acid (HCl, 36.5% - 38%; J.T. Baker), titanium chloride (TiCl₄, 99%; Merck), graphene oxide (rGO) powder, cupric acetate monohydrate (Cu (Ac)₂ · H₂O, 99%; Merck), indium acetate (In (Ac)₃, 99.99%; Sigma Aldrich), octadecylamine (90%;

Merck), thiourea (CS (NH₂)₂, 99%; Sigma Aldrich), silver nitrate (AgNO₃, 99.8%; R&M Chemicals), sodium sulfide (Na₂S, Sigma Aldrich), absolute ethanol, and methanol.

EXPERIMENTAL PROCEDURES

TiO₂ nanoparticles has been synthesized onto cleaned FTO glass using modified hydrothermal method by Han et al. (2015). The 15 mL of deionized (DI) water was mixed with 15 mL of HCl. The mixture was stirred for 5 min followed by 0.5 mL TiCl₄. The mixture was stirred for another 5 min and then placed in a Teflon-lined stainless-steel autoclave. Then, one piece of FTO substrate was placed at an angle against the wall of the Teflon liner with the conductive side facing down. A reaction temperature of 180 °C was used for 10 h reaction time. After synthesis, the autoclave was cooled down to room temperature. Then the FTO substrate was rinsed extensively with DI water and allowed to dry in ambient air. Lastly, annealed at 450 °C for 30 min.

The rGO/CuInS₂ QDs was prepared using modified solvothermal method by Yue et al. (2014). Firstly, 2.5 mg of rGO powder was dispersed in 50 mL absolute ethanol by ultrasonication to obtain a homogeneous suspension. Then, 0.05 mmol of Cu (Ac)₂ · H₂O was dispersed followed by additional of In(Ac)₃ (0.05 mmol) into the dispersion. 0.60 mmol of octadecylamine was ultrasonically dissolved into the dispersion. Next, 0.2 mmol CS(NH₂)₂ was added and a dark-coloured dispersion was produced which also known as CuInS₂ precursor. The CuInS₂ precursor was then transferred into a Teflon-lined stainless-steel autoclave with TiO₂ thin film that placed at an angle against the wall of the Teflon liner with the conductive side facing down. The autoclave was heated at 160 °C for 8 h reaction time. After the autoclave naturally cooled to room temperature, the product was collected by centrifugation (10,000 rpm, 8 min), washed several times with absolute ethanol and dried under N₂ at 60 °C for 3 h.

A modified SILAR technique by Zhang et al. (2015b) was used to deposit Ag₂S layer onto TiO₂/rGO/CuInS₂ thin film. Briefly, TiO₂/rGO/CuInS₂ thin film was dipped into AgNO₃ ethanol solution for 3 min, then rinsed with ethanol. Next, TiO₂/rGO/CuInS₂ thin film was dipped into Na₂S methanol solution and rinsed with methanol. These dipped procedures formed one SILAR cycle and was repeated for 6 SILAR cycles. Lastly, dried under ambient air for an hour.

RESULTS AND DISCUSSION

MORPHOLOGICAL PROPERTIES

Characterization using FESEM was carried out to study the distribution and size of particles of prepared samples.

Based on the observation in Figure 1, it looks like CuInS_2 QDs particles were attached to graphene sheet which covered uniformly the whole surface of TiO_2 film. From the FESEM images, the average particles size of $\text{TiO}_2/\text{rGO}/\text{CuInS}_2$ increased from ± 46.52 to ± 53.97 nm in diameter after Ag_2S deposition as well as the thickness of

the samples which increased from 3.38 to 4.39 μm . These increments were due to the aggregation of Ag_2S particles that formed after the Ag_2S deposition as clearly observed in Figure 2. Basically, larger particle size reduced the gap between the particles, hence reduced the internal surface area of the sample.

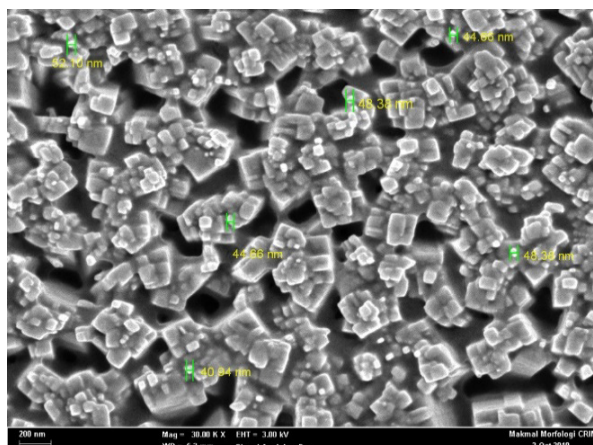


FIGURE 1. Surface morphology of $\text{TiO}_2/\text{rGO}/\text{CuInS}_2$ thin film

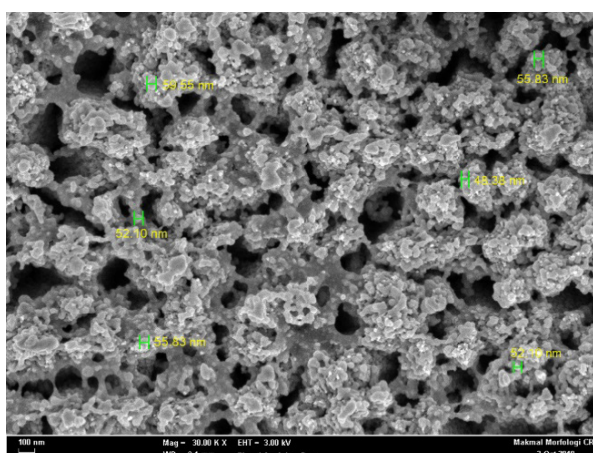


FIGURE 2. Surface morphology of $\text{TiO}_2/\text{rGO}/\text{CuInS}_2$ thin film with Ag_2S deposition layers

Characterization using EDX was performed on $\text{TiO}_2/\text{rGO}/\text{CuInS}_2$ thin film before and after deposition of Ag_2S layers to determine the presence of each element in the samples. From the analysis in Figure 3, Cu, In, and S elements were detected in the spectra which proved that CuInS_2 material were successfully deposited on the TiO_2

thin film surface. While Figure 4 shows the Ag element which proved that Ag_2S layer was successfully applied onto the $\text{TiO}_2/\text{rGO}/\text{CuInS}_2$ thin film. C element that appeared in both spectra shows the existence of graphene in the samples.

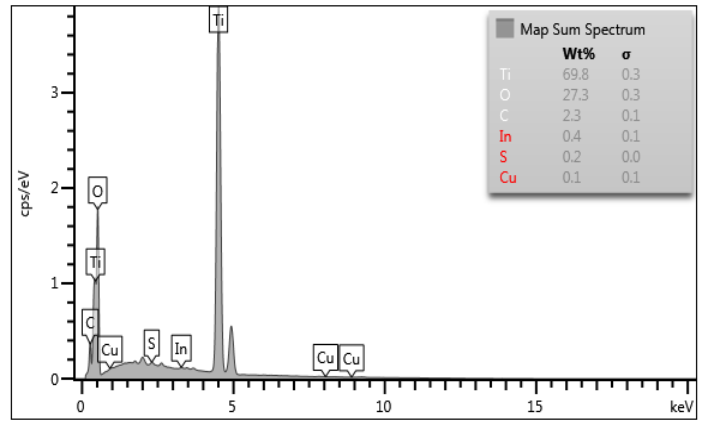


FIGURE 3. EDX spectra of TiO₂/rGO/CuInS₂ thin film

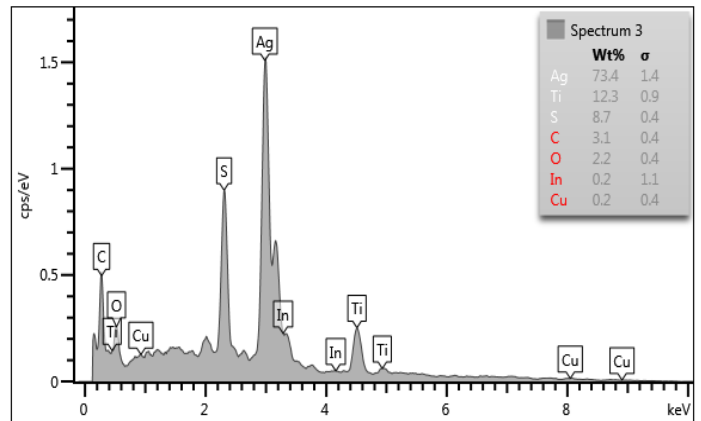


FIGURE 4. EDX spectra of TiO₂/rGO/CuInS₂ thin film with Ag₂S deposition layers

AFM characterization was performed to determine the surface roughness of the TiO₂/rGO/CuInS₂ thin film with and without the Ag₂S coating layer. Based on the AFM images in Figure 5, the RMS value increased after the deposition of Ag₂S layers which showed that Ag₂S were successfully absorbed and cover the surface of the TiO₂/

rGO/CuInS₂ thin film. The RMS value of the TiO₂/rGO/CuInS₂ thin film slightly increased from 10.79 to 11.60 nm with 6 Ag₂S SILAR cycles (Figure 6). The changes in the RMS value indicated that the presence of Ag₂S particles in the sample can be attributed to the increase in particle size of the sample as well.

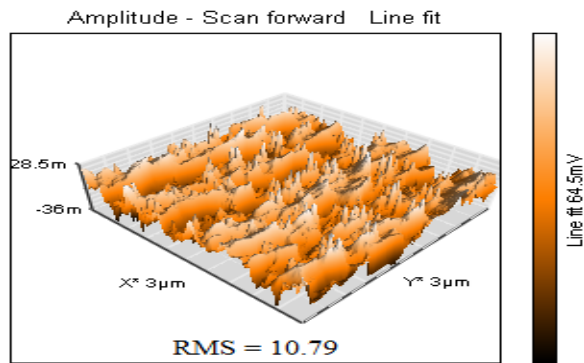


FIGURE 5. Surface roughness of TiO₂/rGO/CuInS₂ thin film

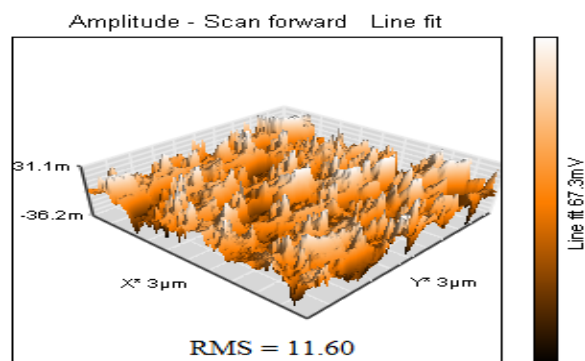


FIGURE 6. Surface roughness of $\text{TiO}_2/\text{rGO}/\text{CuInS}_2/\text{Ag}_2\text{S}$ thin film

STRUCTURAL PROPERTIES

XRD characterization was carried out to identify the structure of TiO_2 , graphene, CuInS_2 , and Ag_2S that could be determined from the crystalline phases of the thin film. The R-labelled peak observed in the XRD spectra refers to TiO_2 at angles of 36.08° corresponding to the plane (101) of the rutile phase (PDF 01-079-5860). For rGO, there is peak at 26.35° corresponding to (002) plane (PDF-01-089-8487). As observed in Figure 7, the typical peaks of rGO was not found in spectra. According to Meng et al. (2015), the disappearance of the (002) diffraction peak of rGO indicates the destruction of the regular stacks of graphene sheets by exfoliation or intercalation of reactants.

Other peaks began to appear after Ag_2S layers were deposited onto the $\text{TiO}_2/\text{rGO}/\text{CuInS}_2$ thin film. There are Ag_2S peaks at angles of 28.97° , 31.52° , 33.61° , 40.74° and 43.41° corresponding to planes (111), (-112), (120), (031) and (200) acanthite phases (PDF 00-011-0688). However, the peaks for CuInS_2 could not be observed in the XRD spectra. This is because TiO_2 and Ag_2S produced crystalline peaks while CuInS_2 produced amorphous peaks. Basically, the crystalline phase has a higher and narrower intensity peak. On the other hand, the amorphous phase has a lower and wider peak intensity. Different peaks in the same spectra cause the amorphous peaks to be less prominent compared to the crystalline peaks. Additionally, there are other peaks present in the spectra that may refer to the FTO glass itself.

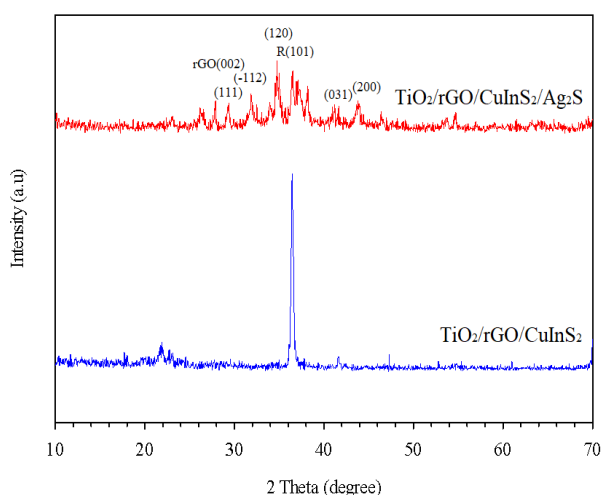


FIGURE 7. XRD spectra of $\text{TiO}_2/\text{rGO}/\text{CuInS}_2$ thin film with Ag_2S deposition layers

The crystallite size of TiO_2 and Ag_2S in $\text{TiO}_2/\text{rGO}/\text{CuInS}_2$ was estimated by Scherrer formula (1). From the calculation, k is the shape constant (0.9), λ is the wavelength of the X-ray (0.15406 nm), β is the FWHM in radians and θ is the Bragg's angle in degree. As stated in

Table 1, the crystallite size of TiO_2 was around ± 33.19 nm to ± 33.97 nm for both samples. While, the crystallite size of Ag_2S in $\text{TiO}_2/\text{rGO}/\text{CuInS}_2$ was estimated to be around ± 19.26 nm.

$$d = \frac{k\lambda}{\beta \cos \theta} \quad (1)$$

TABLE 1. Crystallite size of TiO_2 and Ag_2S using Scherrer equation

Sample	2θ position (deg.)	FWHM (deg.)	Crystallite size (0.01 nm)	
Without Ag_2S	TiO_2	36.08	0.28	33.19
With Ag_2S	TiO_2	36.05	0.27	33.97
	Ag_2S	31.52	0.48	19.26

OPTICAL PROPERTIES

The optical spectrum of the thin film $\text{TiO}_2/\text{rGO}/\text{CuInS}_2$ with and without Ag_2S deposition layers can be observed through UV-VIS Spectroscopy as shown in Figure 8. The significant changes in light absorption can be compared where the absorption of visible light much higher by the QDs structure with the presence of the Ag_2S deposition layer. As the light is absorbed by photosensitizer, the result is an increase in the energy content of the QDs structures. A blue-shift was observed in the electronic properties of the QDs CuInS_2 with the Ag_2S presence. Even though a blue-shift has been typically observed in the literature for shelling of chalcopyrite CuInS_2 (Meng et al. 2015), and it results from the compounding on the surface

between the QDs material and the Ag_2S . Furthermore, a blue-shift can be attributed to the larger particle size of the compound as the Ag_2S layer was deposited. In the meantime, a small red-shift in the absorption region was also detected at the visible edge from the UV-VIS spectra.

In this process, the compound formed has a new band gap energy representative of the ratio of the component materials. However, further studies need to be conducted to identify the materials band gap since the current analysis can only be done up to 700 nm wavelength. Supposedly, the particle size can also be the aspect affecting the band gap of the substantial itself. Therefore, the band gap of $\text{TiO}_2/\text{rGO}/\text{CuInS}_2$ thin film with Ag_2S layers supposed to be narrower than before the Ag_2S deposition.

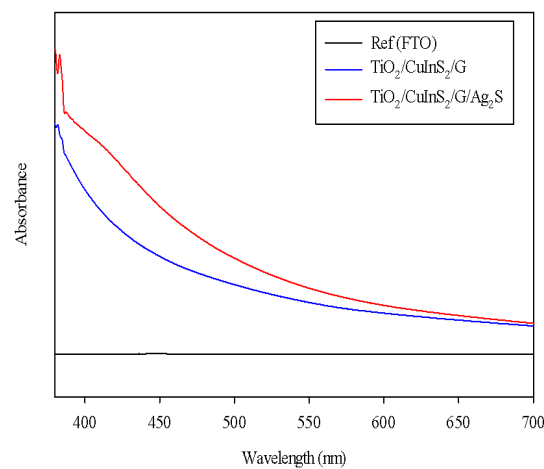


FIGURE 8. UV-VIS spectra of $\text{TiO}_2/\text{rGO}/\text{CuInS}_2$ thin film with Ag_2S deposition layers

ELECTRICAL PROPERTIES

Figure 9 shows the semi-circular curves of electrochemical impedance spectra (EIS) that show the interfacial charge-transfer resistances of the cells. The R_s of the electrodes

in both samples is in the range of 53.3 - 52.1 Ω since both samples used identical FTO substrate, TiO_2 films, and electrolyte. This shows that passivation layer has no effect to the interface combination between FTO substrate and TiO_2 films (Peng et al. 2014).

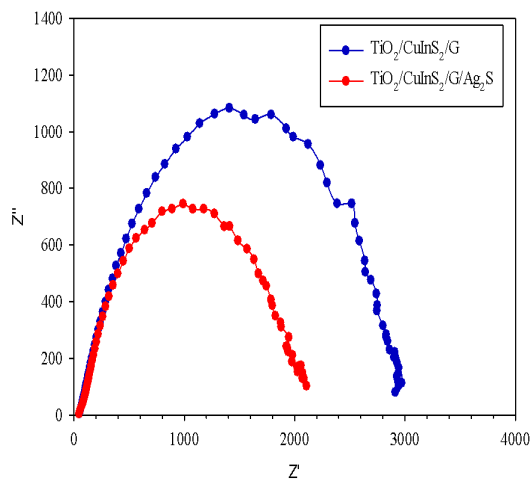


FIGURE 9. EIS spectra of $\text{TiO}_2/\text{rGO}/\text{CuInS}_2$ thin film with Ag_2S deposition layers

However, decrement of semi-circular diameter was observed with the presence of Ag_2S layer. The changes should be ascribed to the charge transfer between TiO_2/QDs interface and/or $\text{QDs}/\text{electrolyte}$ interface. From the EIS spectra, it indicates that the charge transfers resistance decreases with passivation deposition layer (Solaiyammal & Murugakoothan 2019). The lifetime of

the electrons, $\tau_e = 1/(2\pi f_{max})$ where f_{max} is the maximum frequency of the peaks (Tian et al. 2012). The electron lifetime increases with size of the particles as stated in Table 2. According to Ilaiyaraja et al. (2018), due to larger surface defects in smaller sized particles, the electron lifetime might get influenced as well.

TABLE 2. EIS parameters of $\text{rGO}/\text{CuInS}_2$ QDs solar cells

Sample	R_s (Ω)	R_{CT} ($\text{k}\Omega$)	τ_e (ms)
Without Ag_2S	53.3	3.03	1.77
With Ag_2S	52.1	2.14	3.43

Differences in solar cell structure and material will certainly show different performance. Therefore, it is very significant to compare the value of power conversion efficiency for each sample through the I-V curve. In this study, the solar cells comprised redox couple I^-/I_3^- as the electrolyte and Pt glass as the counter electrode with

different photo anodes. The I-V curve was measured under simulated sunlight with active area of 0.25 cm^2 . The performance of the solar cells (V_{oc} , I_{sc} , P_{max} , η) for both samples were specified in detail in Table 3. The efficiency values of the samples studied can be compared and discussed.

TABLE 3. Photovoltaic parameters of the assembled $\text{TiO}_2/\text{rGO}/\text{CuInS}_2$ and $\text{TiO}_2/\text{rGO}/\text{CuInS}_2/\text{Ag}_2\text{S}$ solar cells

Sample	V_{oc} (V)	J_{sc} (mA cm^{-2})	FF	η (%)
Without Ag_2S	0.376	0.356	0.55	0.074
With Ag_2S	0.410	1.676	0.48	0.330

As expected, the presence of the Ag_2S layer helps in enhance the efficiency of photovoltaic power conversion. From the I-V curve as shown in Figure 10, obvious increment observed for $\text{TiO}_2/\text{rGO}/\text{CuInS}_2$ photo anode with Ag_2S layers compared to the other sample. Compared to $\text{TiO}_2/\text{rGO}/\text{CuInS}_2$ photo anode with Ag_2S deposition layers produced higher value of power conversion

efficiency, 0.33% with higher value of I_{sc} and FF , 0.419 mA and 48%, respectively. It proved that $\text{TiO}_2/\text{rGO}/\text{CuInS}_2/\text{Ag}_2\text{S}$ have better capability in electrical conductivity and electron mobility than $\text{TiO}_2/\text{rGO}/\text{CuInS}_2$. As the result, solar cell performance improved with the presence of the Ag_2S deposition layers compared to the sample without the Ag_2S passivation layers.

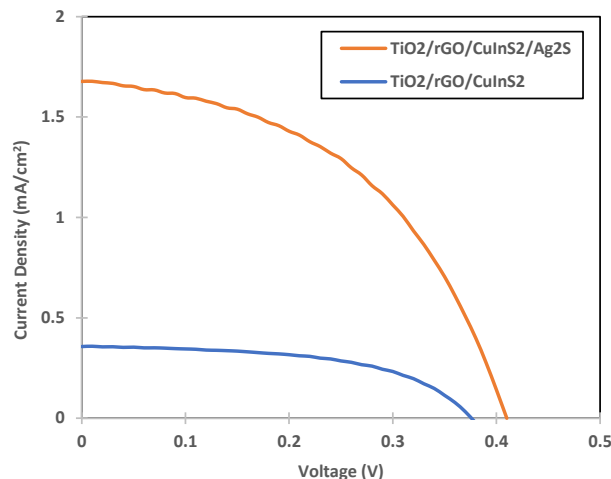


FIGURE 10. J - V curve of $\text{TiO}_2/\text{rGO}/\text{CuInS}_2$ thin film with and without Ag_2S deposition layers

CONCLUSION

Ag_2S layers has been successfully deposited onto $\text{TiO}_2/\text{rGO}/\text{CuInS}_2$ thin film using SILAR technique. The effect of Ag_2S on the photovoltaic performance of $\text{rGO}/\text{CuInS}_2$ based QDSSCs was investigated. From FESEM images, the average particles size of the samples ranged from ± 46.52 to ± 53.97 nm in diameter. The XRD results showed peaks at 33.61° , 40.74° and 43.41° of Ag_2S structure and the crystallite size of Ag_2S was estimated around ± 19.26 nm. According to UV-VIS analysis, $\text{TiO}_2/\text{rGO}/$

CuInS_2 showed better light absorption capability with the presence of Ag_2S layers. Regarding the considerable results obtained, it was pointed out that $\text{TiO}_2/\text{rGO}/\text{CuInS}_2$ with Ag_2S as passivation layer can be introduced as an effective photo anode for making efficient QDSSCs devices with 0.33% of power conversion efficiency. Therefore, for further investigation, other characterizations should be carried out in order to prove the influence of Ag_2S layers in enhancement of the $\text{rGO}/\text{CuInS}_2$ based QDSSCs performance.

ACKNOWLEDGEMENTS

The authors would like to acknowledge the financial assistance provided (Grant No.: 07-01-02-SF1388) by the Ministry of Energy, Science, Technology, Environment and Climate Change (MESTECC). Besides, the authors are thankful to the supports received from Solar Energy Research Institute (SERI) and Center for Research and Instrumentation Management (CRIM), Universiti Kebangsaan Malaysia (UKM).

REFERENCES

- Han, M., Jia, J., Yu, L. & Yi, G. 2015. Fabrication and photoelectrochemical characteristics of CuInS₂ and PbS quantum dot co-sensitized TiO₂ nanorod photoelectrodes. *RSC Advances* 5(64): 51493-51500.
- Holi, A.M., Zainal, Z., Talib, Z.A., Lim, H.N., Yap, C.C., Chang, S.K. & Ayal, A.K. 2017. Enhanced photoelectrochemical performance of ZnO nanorod arrays decorated with CdS shell and Ag₂S quantum dots. *Superlattices and Microstructures* 103(2017): 295-303.
- Hosseinpour-Mashkani, S.M., Salavati-Niasari, M. & Mohandes, F. 2014. CuInS₂ nanostructures: Synthesis, characterization, formation mechanism and solar cell applications. *Journal of Industrial and Engineering Chemistry* 20(5): 3800-3807.
- Ilaiyaraja, P., Rakesh, B., Das, T.K., Mocherla, P.S. & Sudakar, C. 2018. CuInS₂ quantum dot sensitized solar cells with high VOC ≈ 0.9 V achieved using microsphere-nanoparticulate TiO₂ composite photoanode. *Solar Energy Materials and Solar Cells* 178: 208-222.
- Kouhnavard, M., Ikeda, S., Ludin, N.A., Khairudin, N.A., Ghaffari, B.V., Mat-Teridi, M.A., Ibrahim, M.A., Sepeai, S. & Sopian, K. 2014. A review of semiconductor materials as sensitizers for quantum dot-sensitized solar cells. *Renewable and Sustainable Energy Reviews* 37(2014): 397-407.
- Kumari, A., Singh, I., Prasad, N., Dixit, S.K., Rao, P.K., Bhatnagar, P.K., Mathur, P.C., Bhatia, C.S. & Nagpal, S. 2014. Improving the efficiency of a poly(3-hexylthiophene)-CuInS₂ photovoltaic device by incorporating graphene nanopowder. *Journal of Nanophotonics* 8 (1): 083092.
- Madhavan, A.A., Kalluri, S., Chacko, D.K., Arun, T.A., Nagarajan, S., Subramanian, K.R., Nair, A.S., Nair, S.V. & Balakrishnan, A. 2012. Electrical and optical properties of electrospun TiO₂-graphene composite nanofibers and its application as DSSC photo-anodes. *RSC Advances* 2(33): 13032-13037.
- Meng, W., Zhou, X., Qiu, Z., Liu, C., Chen, J. & Yue, W. 2015. Reduced graphene oxide-supported aggregates of CuInS₂ quantum dots as an effective hybrid electron acceptor for polymer-based solar cells. *Carbon* 96: 532-540.
- Mustakim, N.S.M., Ubani, C.A., Sepeai, S., Ludin, N.A., Teridi, M.A.M. & Ibrahim, M.A. 2018. Quantum dots processed by SILAR for solar cell applications. *Solar Energy* 163(2018): 256-270.
- Peng, Z., Liu, Y., Zhao, Y., Chen, K., Cheng, Y., Kovalev, V. & Chen, W. 2014. ZnSe passivation layer for the efficiency enhancement of CuInS₂ quantum dots sensitized solar cells. *Journal of Alloys and Compounds* 587(2014): 613-617.
- Solaiyammal, T. & Murugakoothan, P. 2019. Green synthesis of Au and the impact of Au on the efficiency of TiO₂ based dye sensitized solar cell. *Materials Science for Energy Technologies* 2(2): 171-180.
- Tian, J., Gao, R., Zhang, Q., Zhang, S., Li, Y., Lan, J., Qu, X. & Cao, G. 2012. Enhanced performance of CdS/CdSe quantum dot cosensitized solar cells via homogeneous distribution of quantum dots in TiO₂ film. *The Journal of Physical Chemistry C* 116(35): 18655-18662.
- Tubtimtae, A., Wu, K.L., Tung, H.Y., Lee, M.W. & Wang, G.J. 2010. Ag₂S quantum dot-sensitized solar cells. *Electrochemistry Communications* 12(9): 1158-1160.
- Ubani, C.A., Ibrahim, M.A., Teridi, M.A.M., Sopian, K., Ali, J. & Chaudhary, K.T. 2016. Application of graphene in dye and quantum dots sensitized solar cell. *Solar Energy* 137: 531-550.
- Yue, W., Lan, M., Zhang, G., Sun, W., Wang, S. & Nie, G. 2014. Size-dependent polymer/CuInS₂ solar cells with tunable synthesis of CuInS₂ quantum dots. *Materials Science in Semiconductor Processing* 24(2014): 117-125.
- Zhang, R., Qi, S., Jia, J., Torre, B., Zeng, H., Wu, H. & Xu, X. 2015a. Size and refinement edge-shape effects of graphene quantum dots on UV-visible absorption. *Journal of Alloys and Compounds* 623(2015): 186-191.
- Zhang, X., Liu, J., Zhang, J., Vlachopoulos, N. & Johansson, E.M. 2015b. ZnO@Ag₂S core-shell nanowire arrays for environmentally friendly solid-state quantum dot-sensitized solar cells with panchromatic light capture and enhanced electron collection. *Physical Chemistry Chemical Physics* 17(19): 12786-12795.

Nurul Syafiqah Mohamed Mustakim
Spectrum International College of Technology
2F-26A, The Main Place Mall
Jalan USJ21/10, USJ 21
47360 Subang Jaya, Selangor Darul Ehsan
Malaysia

Nurul Syafiqah Mohamed Mustakim, Muhazri Abd Mutalib, Suhaila Sepeai, Norasikin Ahmad Ludin, Mohd Asri Mat Teridi & Mohd Adib Ibrahim*
Solar Energy Research Institute (SERI)
Universiti Kebangsaan Malaysia
43600 UKM Bangi, Selangor Darul Ehsan
Malaysia

*Corresponding author; email: mdadib@ukm.edu.my

Received: 12 August 2020

Accepted: 27 August 2020